Materials Properties of Ultra-Incompressible Re_2P

Sebastian B. Schneider,[1] Dominik Baumann,[1] Ashkan Salamat,[2] Zuzana Konôpková,[3] Hanns-Peter Liermann,[3] Marcus R. Schwarz,[4] Wolfgang Morgenroth,[5] Lkhamsuren Bayarjargal,[5] Alexandra Friedrich,[5] Björn Winkler,[5] and Wolfgang Schnick*[1]

[1] *Department Chemie, Ludwig-Maximilians-Universität, 81377 München, Germany*

[2] *The European Synchrotron Radiation Facility (ESRF), 38000 Grenoble, France*

[3] *Deutsches Elektronen Synchrotron (DESY), 22607 Hamburg, Germany*

[4] *Freiberger Hochdruckforschungszentrum, Institut für Anorganische Chemie, Leipziger Straße 29, 09599 Freiberg, Germany.*

[5] *Institut für Geowissenschaften, Abt. Kristallographie, Goethe-Universität Frankfurt, 60438 Frankfurt a. M., Germany*

KEYWORDS Bulk modulus, Vickers hardness, Diamond-anvil cell technique, Synchrotron radiation, Phosphide

Supporting Information

ABSTRACT: *In situ* high-pressure X-ray powder diffraction measurements on Re_2P up to 37.0 GPa at ambient temperature in diamond-anvil cells were carried out at two different synchrotron facilities (ESRF and DESY). The compressibility of Re_2P (*Pnma*, no. 62, a = 5.5464(17), b = 2.9421(8), c = 10.0483(35) Å, V = 163.97(9) Å^3, Z = 4, R_p = 0.1008, wR_p = 0.1341 at ambient conditions) was investigated and resulted in a bulk modulus of B_0 = 320(10) GPa after fitting the experimental p–V data to a second- and third-order Birch-Murnaghan equation of state. In addition, the determined bulk modulus is compared to values obtained from an Eulerian strain versus normalized stress plot with values ranging form 315(7) to 321(15) GPa. These experimental findings are confirmed by DFT-calculations ranking Re_2P amongst ultra-incompressible materials. However, the Vickers hardness of a high-pressure sintered Re_2P-Re_xC_y composite material in the asymptotic hardness region was found to be of only 13(2) GPa. Electrical conductivity measurements indicate that metallic Re_2P exhibits Pauli-paramagnetism. Analysis of temperature-dependent *in situ* X-ray diffractometry reveals an approximately isotropic expansion of the lattice parameters with a thermal expansion coefficient of ($\alpha(V) = 28.5–32.8(2)\cdot10^{-6}$ K^{-1}).

Introduction

The search for superhard and ultra-incompressible materials is of great interest and importance in science and technology because these materials find applications for coatings on cutting tools or as abrasives and polishing media. Despite significant advances in the field of synthesis of very hard materials diamond is still considered to be the hardest material when considering its Vickers hardness (60–150 GPa)[1-5] as well as its bulk modulus (433–442 GPa).[1-4,6,7] These properties are ascribed to the directional bonding in covalent networks of atoms coordinated by a small number of ligands with short interatomic distances. So called low Z compounds consisting of atoms with small atomic numbers, such as Be, B, C, N, O, Al, Si or P fulfill these criteria. Incorporation of heteropolar atoms with increasing ionic radii results in the formation of binary or multinary compounds that show a decreasing covalent character, which can be ascribed to the formation of longer and more ionic bonds. This usually results in a reduced hardness and a higher compressibility of the corresponding materials as compared to diamond.

More recently, novel compounds of transition metals with a very high valence electron density from groups IV to X in combination with low Z elements raised considerable interest because they could exhibit both, high hardness and extremely high bulk moduli. OsB_2, WB_2, WB_4, Re_2C, WC, PtC, MN_2 (M = Os, Ir, Pt), Re_2N or Re_3N with ultrahigh bulk moduli (428 GPa for IrN_2) are only a few members of this group of compounds.[4,8-16] The origin of the unusual properties is the complex bonding situation found in these transition metal borides, carbides or nitrides: metal-metal, nonmetal-metal and nonmetal-nonmetal interactions with covalent character. Therefore, the combination of low Z elements (forming strong, directional bonds) with transition metals (with a high valence electron density that resists deformation) is a promising mixture for the synthesis of novel materials with interesting properties. However, further detailed analysis of the hardness of these new materials was so far not possible because their synthesis in diamond-anvil cells produced only very small sample amounts. Thus, their true hardness is still unknown.

However, the physical properties of hardness and incompressibility of materials with slightly heavier low Z elements (e.g. silicon, phosphorus or sulfur) have not yet been investigated in detail because values for hardness and incompressibility are thought to be lower than expected if compared to the incorporation of B or N. Here, we report the synthesis and

characterization of a transition metal phosphide, Re_2P. Compressibility, hardness, magnetic properties and electrical conductivity as well as the thermal expansion were determined. By incorporation of phosphorus (low *Z* element) into elemental rhenium (which exhibits a bulk modulus of about 367 GPa)[17] interesting properties are expected.

Experimental Section

Synthesis of Re_2P. The crystal structure of Re_2P has already been characterized by Rühl *et al.* a few years ago.[18] These authors were able to synthesize single crystals of Re_2P in an evacuated silica tube at 1200 K starting with a stoichiometric mixture of the elements and tin in excess acting as flux. The phosphorus containing tin-rich matrix was then dissolved in moderately diluted, hot hydrochloric acid, yielding black, metallic single crystals of Re_2P.

Adopting the reported synthesis route, we also obtained Re_2P but as powder. Starting materials for the synthesis of bulk and phase-pure Re_2P were rhenium powder (smart-elements, 99.95%), semiconductor-grade red phosphorus (Merck, for synthesis) and tin (Merck, fine powder, particle size < 71 μm). In a sealed silica tube under argon atmosphere, the initial mixture with composition Re:P:Sn = 2:1:12 was heated from ambient temperature to 1200 K with 1 K/min, annealed for 7 days and then cooled down to ambient temperature within 5 days. After dissolving the tin-rich matrix in half-concentrated, hot HCl black, coarsely grained metallic Re_2P was obtained. The solid was filtered and dried at 400 K for 24 hours. Energy dispersive X-ray spectroscopy and X-ray powder diffraction of the samples confirmed the successful synthesis of Re_2P. The powder X-ray diffraction pattern was recorded with a STOE Stadi P powder diffractometer (STOE, Germany) in Debye-Scherrer geometry using Ge(111) monochromated Mo-$K_{\alpha1}$-radiation (0.7093 Å). The energy-dispersive X-ray spectra were obtained with a SM-6500F scanning electron microscope (JEOL, Germany).

***In situ* X-ray powder diffraction.** *In situ* powder X-ray diffraction experiments at high pressure were carried out on beamline ID27 at the ESRF.[19] A Boehler-Almax diamond-anvil cell equipped with 300-μm culet diamonds and a rhenium gasket was used and the pressure increased manually.[20] The gasket was pre-indented to 42 μm and a 120-μm hole to hold the sample was drilled into the gasket using a Nd:YAG laser. Helium pre-compressed to 1800 bar was pressed into the sample chamber and served as the pressure transmitting medium (PTM). The powder sample was surrounded by three ruby spheres. The pressure was determined by ruby fluorescence measurements using the calibration of Mao *et al.*.[21] Monochromatic radiation with a wavelength of λ = 0.3738 Å (E = 55.04 keV) was selected. The beam was focused on a 3 x 3 μm^2 area and a total number of 11 diffraction images were collected at pressures ranging from 6.4 to 20.9 GPa. The pressure at each diffraction image was measured before and after the data collection and averaged to its final value. Diffracted intensities were recorded with a MAR165 CCD detector. Exposure times were typically between 5 to 20 seconds, depending on saturation of the detector. To average the texture the cell was oscillated by ± 10° relative to the incident beam. A precise calibration of the detector parameters was performed with LaB_6 powder as reference material. The diffraction images were processed and integrated using the program Fit2D.[22]

Additional *in situ* X-ray powder diffraction experiments at high pressure were carried out at the Extreme Conditions Beamline (ECB) P02.2 at the PETRA III, DESY.[23] A membrane driven symmetric diamond-anvil cell equipped with 400-μm culet diamonds and a rhenium gasket was used with an automated pressure controller.[24] The gasket was pre-indented to 43 μm and a 160-μm hole drilled with a Nd:YAG laser to contain the sample. Neon pre-compressed to 1500 bar was pressed into the sample chamber and served as the PTM. The powder sample was surrounded by three ruby spheres. The pressure was determined through the ruby fluorescence scale by Mao *et al.*[21] using the offline Fluorescence spectrometer of the Extreme Conditions Science Infrastructure (ECSI) at PETRA III. Monochromatic radiation with a wavelength of λ = 0.29036 Å (E = 42.75 keV) was selected. The beam was focused to less than 2 x 2 μm and a total number of 36 diffraction images were collected at pressures ranging from 3.0 to 37.0 GPa. The pressure at each diffraction image was measured before and after the data collection and averaged to its final value. Diffracted intensities were recorded with a XRD1621 ScI/amorphous silicon area detector from Perkin Elmer. Exposure times were typically 15 to 30 seconds. To average on texture the DAC was oscillated by ± 4° relative to the beam. A precise calibration of the detector parameters was performed with CeO_2 powder (NIST) as reference material. The diffraction images were processed and integrated using the programs GSE_Shell and Fit2D.[22,25]

Rietveld refinement of high-pressure data. The Rietveld refinement of Re_2P at ambient and extreme conditions was performed with the TOPAS-Academic package[26] (see Figure 1). The crystallographic parameters for Re_2P at ambient conditions were taken from the literature[18] and fitted to the powder X-ray pattern obtained after synthesis. These crystallographic parameters were taken as starting values for the Rietveld refinements of data collected at higher pressures. The reflection profiles were determined using the fundamental parameters approach[27] by convolution of appropriate source emission profiles with axial instrument contributions and crystalline microstructure effects. Preferred orientation of the crystallites was described with a spherical harmonics function of 8th order. No structural phase transition was observed up to the maximum applied pressure of 37.0 GPa.

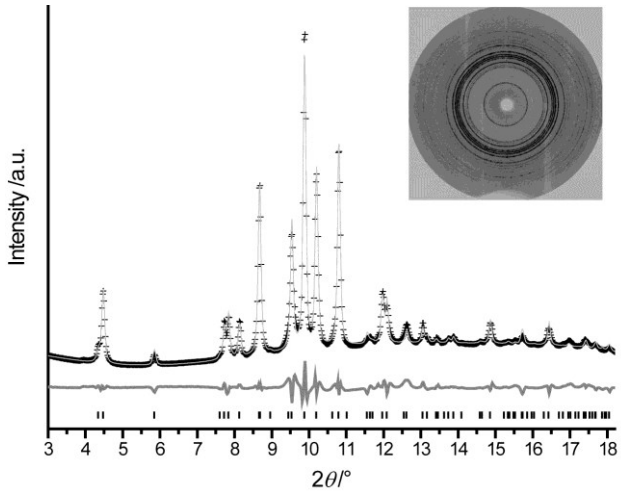

Figure 1. Observed (crosses) and calculated (upper gray line) diffraction pattern as well as difference profile of the Rietveld refinement of Re_2P at 15.1 GPa (ESRF); peak positions of Re_2P

are marked by vertical lines; two-dimensional image plate data at the upper right.

Equation of state. The isothermal bulk modulus B_0 and its pressure derivative B' for Re_2P were obtained from fits of a second- and third-order Birch–Murnaghan (BM) equation of state (EoS)[28,29] to the p–V data at 300 K:

$$p = 3B_0 f(1 + 2f)^{5/2} \times [1 + 3/2(B' - 4)f], \quad (1)$$

$$\text{where } f = [(V/V_0)^{-2/3} - 1]/2 \quad (2)$$

represents the Eulerian strain, where V_0 is the volume at zero pressure, so

$$p = 3/2B_0[(V/V_0)^{-7/3} - (V/V_0)^{-5/3}] \times \{1 - 3/4(4 - B')[(V/V_0)^{-2/3} - 1)]\}. \quad (3)$$

For B' fixed to 4, the second-order BM-EoS is obtained. To check the quality of the EoS fit, the BM-EoS was also expressed in terms of the Eulerian strain f and the normalized pressure F

$$F = p/3f(1 + 2f)^{5/2}. \quad (4)$$

The compression data are therefore additionally presented in a $F(f)$-plot,[30] where the intercept with the F-axis yields B_0, whereas the slope is $3\times B_0(B' - 4)/2$ and thus provides B'.

$$F = B_0 + [3B_0(B' - 4)f]/2. \quad (5)$$

The $F(f)$ form of representation of the p–V data is very sensitive to scattering of data and to experimental uncertainties as the bulk modulus and its first pressure derivative are obtained by a linear fit.[29] All expressions of B_0 and B', the second- and third-order BM-EoS fits and the $F(f)$-plot calculations were done using the software Origin.[31] For all calculations the error in pressure was set to 0.5 GPa.

Computational details. Density functional theory, DFT, based calculations were performed with academic and commercial versions of the CASTEP program[32–34] using a generalized gradient approximation in the PBESOL formulation.[35] For all calculations ultrasoft pseudopotentials from the CASTEP data base were generated "on the fly", with 5 and 15 valence electrons for P and Re, respectively. The maximum cutoff energy of the plane waves was 330 eV. In addition to the cutoff energy, the quality of the calculations is determined by the density of the grid of k-points in the Brillouin zone. Here distances between the points were less than 0.03 $Å^{-1}$. The wave vectors for the sampling points were chosen according to the scheme proposed in the literature.[36] Full geometry optimization calculations were performed. Structures were considered to be converged when the largest residual component of the stress tensor was less than 0.02 GPa and the largest residual force acting on an atom was less than 0.01 eV/Å. The elastic stiffness coefficients were obtained as the proportionality constants between the applied strains and the resultant stresses. Strain patterns were imposed with several magnitudes up to a distortion of 0.2 % of the lattice parameters, and after geometry optimization of the internal parameters the resultant stresses were computed. The present calculations are restricted to the athermal limit, in which temperature effects and zero-point motions were neglected.

Vickers hardness measurements. For the Vickers hardness measurements Re_2P was sintered at 4 GPa and 700 K in a modified Walker-type module in combination with a 1000 t multianvil press (both devices from Voggenreiter, Germany). As pressure media, MgO-octahedra (Ceramic Substrates & Components, UK) with edge lengths of 18 mm (18/11 assembly) were employed. Eight tungsten carbide cubes (2050 HV 30, Hawedia, Germany) with truncation edge lengths of 11 mm compressed the octahedra. Re_2P was filled into a cylindrical boron nitride crucible (Henze BNP GmbH, Germany) and sealed with a fitting boron nitride plate. Details of the setup are described in the literature.[37–40] Phase-purity of as-sintered Re_2P was confirmed by powder X-ray diffractometry in reflection geometry. A cylindrical piece of Re_2P was then transferred into a copper tube, fixed with epoxy based adhesive and cut into 1.5 mm thick slices with a diamond wire. This assembly was placed in the center of an alumina ring with 10 mm outer diameter in order to maintain planarity during the following polishing process and then further warm-embedded into a thermoplastic acrylic resin. The samples were then subsequently wet-ground with silicon carbide paper and finally polished with a 3 μm diamond suspension.

The Vickers hardness was measured over a range of loads (0.0025–0.5 kg indentation load) using a FM-300 microhardness tester (Future-Tech Corp., Japan). Additional indents at a load of 1 kg were made with a Buehler MACROMET tester (Buehler GmbH, Germany). The loads were applied for 10 s. For each load, at least four indentations were made and each indentation was measured twice under slightly different focal conditions. The measurement of the indentation diagonals was performed with an optical microscope at 500× magnification in combination with a CCD-camera and the Minuteman™ software package (Fritz Müller GmbH, Germany). The Vickers Hardness (in Gigapascal) was calculated according to $HV = 1854.4 \cdot g \cdot L/\langle d \rangle^2$, where g is the gravitational acceleration, L the load in kg and $\langle d \rangle$ the averaged indentation diagonal in μm. The constant on the right hand side of the equation accounts for the ratio between the surface and the base of the Vickers pyramid and contains additional scaling factors for the chosen units.

Magnetic and conductivity measurements. The magnetic measurements were performed on a Quantum Design MPMS XL5 SQUID magnetometer. Resistivity (and conductivity) were determined from a cold pressed (10 kN) pellet of non-sintered Re_2P (diameter: 5mm, thickness: 1mm) using the four probe method. The pellet was mounted onto a brass template and its remaining surface contacted with four equidistant probes. A current of 10^{-3} A was applied and the potential difference was measured as a function of the temperature (ambient temperature to 10 K) yielding the specific resistance (and conductivity) according to Ohm's law. No superconductivity was observed.

Thermal expansion analysis. *In situ* X-ray powder diffraction data were collected with a STOE Stadi P powder diffractometer (Mo-$K_{\alpha 1}$-radiation (0.7093 Å)) equipped with a computer controlled STOE resistance graphite furnace. Enclosed in a silica glass capillary, non-sintered samples were heated from ambient temperature to 1250 K in 5 K/min in steps of 25

K. At each heating step (after holding the temperature for 1 minute), a diffraction pattern was recorded with an IP-PSD in the range of $2° \leq 2\theta \leq 80°$. To determine the cell parameters at different temperatures accurately for all diffraction patterns a Rietveld refinement has been performed for every temperature step. Finally, according to equation [(6)], the average thermal expansion coefficient α was determined:

$$\alpha = 1/X_0(\partial X/\partial T)_p, \quad (6)$$

where X denotes the lattice parameter or cell volume, T is temperature and subscript 0 refers to the data at room temperature.

To check the quality of the data, the expansion coefficient was also determined automatically with a thermo-mechanic analyser TMA 402 *Hyperion*® (NETSCH, Selb, Germany). The expansion of sintered Re_2P with cylindrical shape was measured under helium atmosphere between 250 and 1250 K with a heating rate of 3 K/min yielding the relative expansion $\Delta L/L$ and the linear thermal expansion coefficient α.

Results and Discussion

Crystal structure elucidation. Re_2P crystallizes in space group *Pnma* (no. 62) isotypic with Co_2P-type structures.[18,41] The refined structural parameters at ambient conditions and at the maximum applied pressure of 37.0 GPa are shown in Table S1 and are compared to the obtained values of the DFT-calculation. In Figure 2, the unit cell at ambient conditions is displayed in [100], [010] and [001] directions to illustrate the stacking order of all atoms. In the [100] direction there are puckered Re-Re and Re-P strands, whereas in the [001] direction a straight Re-Re-P stacking is observed. Only in the [010] direction, linear strands of Re and P atoms can be found. The shortest Re-P distances at ambient conditions and at 37.0 GPa are summarized in Table 1 and an evolution of the normalized lattice parameters with pressure is illustrated in Figure 3.

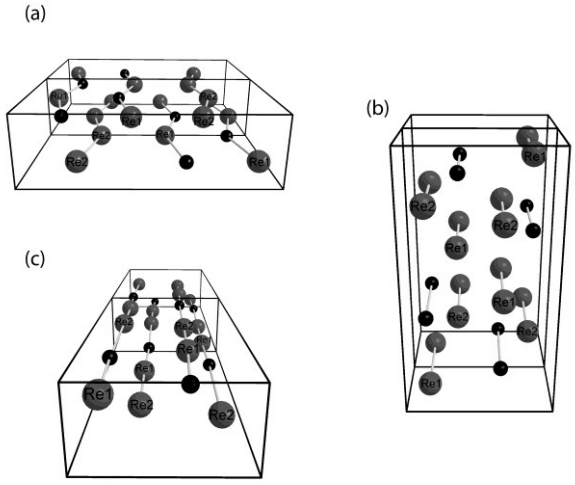

Figure 2. Doubled unit cell of Re_2P at ambient conditions in (a) [100], (b) [010] and (c) [001] direction. Pale lines between atoms illustrate stacking of atoms: Rhenium gray, phosphorus black.

Table 1. Shortest experimental Re-Re distances at ambient conditions and at 37.0 GPa (DESY) in Å. The second line for each distance, set in italics, gives the corresponding values from the DFT-PBESOL calculations. Only the shortest distances within one stacking are listed. The Re-Re distances in elemental Re are 2.760 Å in [100] and [010] (both linear strands) and 2.747 Å in [001] direction (puckered).[42]

Direction and sort	Ambient conditions	37.0 GPa
Re-Re in [100]	2.8505(7)	2.7687(1)
	2.8534	*2.7764*
Re-Re in [010]	2.9421(8)	2.8357(3)
	2.9215	*2.8184*
Re-Re in [001]	2.7968(30)	2.7398(88)
	2.7870	*2.7125*

Due to the orthorhombic unit cell, the compression of the axes shows interesting anisotropy. The *b*-direction of the crystal is most compressible, while the *a*-direction is the least compressible. This observation can be understood if the shortest Re-Re distances are taken into account. These distances are most probably the limiting factor during compression of the lattice because the shorter the distance of the atoms at ambient conditions the less shortening can be expected during compression due to quickly increasing repulsive forces. Since the shortest Re-Re distance is observed along [100], the corresponding lattice parameter is the least compressible.

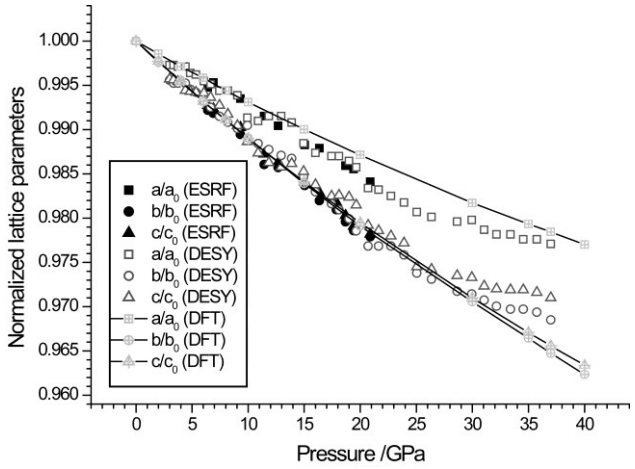

Figure 3. Evolution of normalized lattice parameters of Re_2P with pressure. The lattice parameters at zero pressure (ESRF and DESY) were taken from the Rietveld refinement of the powder X-ray pattern measured after synthesis with Mo-$K_{\alpha 1}$-radiation.

EoS analysis. Fits of a second- and third-order Birch-Murnaghan equation of state to the experimental and theoretical *p*–*V* data are presented in Figure 4(a), 4(c) and 4(e) (ESRF, DESY, DFT-PBESOL). The corresponding linear fits of the *F*(*f*) plot are illustrated in Figure 4(b), 4(d) and 4(f). The results of the fits are summarized in Table 2.

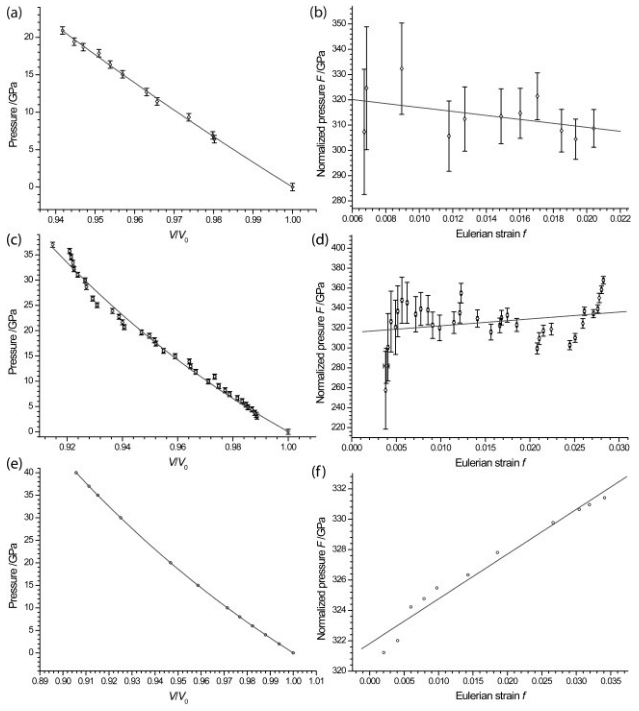

Figure 4. (a) and (c): third-order Birch-Murnaghan fits (gray line) to the experimental *p*–*V* data of Re_2P; (b) and (d): *F*(*f*)-plot with linear fits (gray line) to the applied values of the third-order BM-EoS; (e) and (f): corresponding fits to the DFT-calculated *p*–*V* data. Top: ESRF (pressure medium: He), middle: DESY (pressure medium: Ne); bottom: DFT-PBESOL.

The experimentally obtained bulk modulus of Re_2P for all fits ranges in between 304–333 GPa. However, the strong scattering and huge error bars of the data in the *F*(*f*) plots and the deviation of the value of the first pressure derivative *B´* from 4 after fitting a BM-Eos of third-order to the experimental *p*–*V* data, might be a direct consequence of non-hydrostatic conditions and demand a theoretical confirmation of the calculated bulk modulus. These density functional theory based findings are in very good agreement with the experimental values and give a bulk modulus of 321(1) GPa from the elastic stiffness coefficients and a bulk modulus of 322.9(2) GPa from a fit of a BM-EoS of 3rd order. Therefore, the experimental bulk modulus can be considered as appropriate classifying Re_2P amongst ultra-incompressible materials.

Table 2. Bulk moduli B_0 and first pressure derivatives *B´* of Re_2P obtained from second- and third-order Birch-Murnaghan EoS and normalized strain fits to experimental and theoretical *p*–*V* data.

	BM 2nd	BM 3rd	Natural Strain 3rd
ESRF			
B_0 (GPa)	311.6(1.9)	327.1(8.9)	321.8(14.9)
B ’	4 (fixed)	2.1(1.0)	2.5(0.2)
DESY			
B_0 (GPa)	333.2(3.2)	304.0(12.9)	315.3(7.3)
B ’	4 (fixed)	6.7(1.4)	5.5(0.7)
DFT-PBESOL			
B_0 (GPa)	330.2(5)	322.9(2)	321.8(4)
B ’	4 (fixed)	4.5(0)	4.7(6)

The observed range of the bulk modulus for Re_2P is extremely high, exceeding or matching other hard materials like B_4C (B_0 = 200 GPa), Si_3N_4 (B_0 = 249 GPa) and stishovite-type SiO_2 (B_0 = 305–316 GPa).

Vickers hardness and microstructure. The variation of hardness with load is given in Figure 5. The hardness of both samples shows a very steep decrease at loads above 50 g and then decreases at a lower rate from ~15 GPa at 100 g down to around 12 GPa at 1 kg load.

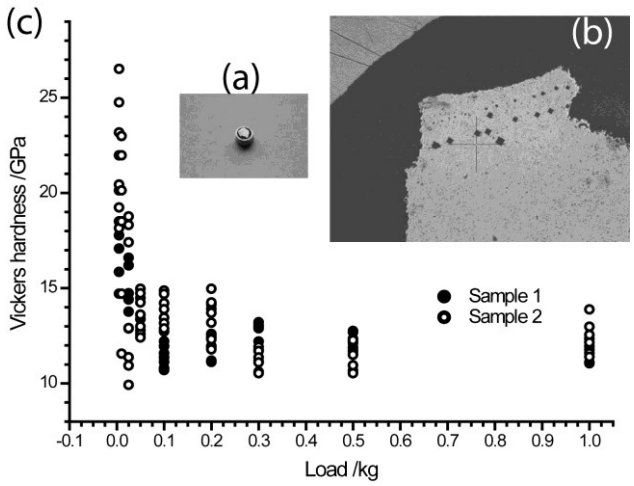

Figure 5. Sintered and polished Re_2P embedded in epoxy based adhesive and copper cylinder. (b) Indentations at various loads. (c) Resulting Vickers hardness at corresponding loads.

In general, the indentation hardness reading depends on the material resistance to a local plastic (i.e. remanent) deformation. However, it is known that a partial elastic recovery of the sample usually takes place once the indenter is removed.[43,44] At considerably low loads, the relative part of the compression energy consumed by the elastic deformation increases significantly. Thus, the measured hardness increases with the load decrease. This phenomenon is observed for both metals and ceramics and referred to as indentation size effect (ISE).[45,46] The ISE is not only due to an elastic recovery alone but to a complex combination of different material and measurement technique related factors. As the employed indenters have been previously used for hardness testing of ultrahard materials, an enhanced blunting of their tip and therefore deviation from their ideal geometry may have also contributed to the observed ISE.

Because of the ISE, it is usually suggested to perform hardness measurements through a wide range of loads, in order to

find the load conditions where the major part of the deformation energy is spent on plastic deformation of the material. Under such conditions the hardness is almost load-independent and is usually referred to as the true hardness.[44,47,48] Thus, the averaged Vickers hardness obtained from the high load data is 13(2) GPa. Closer investigation of the surface of polished Re_2P using SEM/EDX revealed that the sintered samples had some residual porosity, but also showed regions of different phosphorus and additional carbon content (see Figure 6). Comments on the microstructure and composition of as-sintered Re_2P can be found in the Supporting Information.

In summary, it has to be stated that the determined Vickers hardness refers not to phase-pure Re_2P and dense rather than to a slightly porous Re_2P-Re_xC_y composite material. Nevertheless, we assume that the actual hardness of phase-pure Re_2P will not be dramatically different, at least for large indents, where the effect of the harder Re_xC_y and residual porosity may cancel each other.

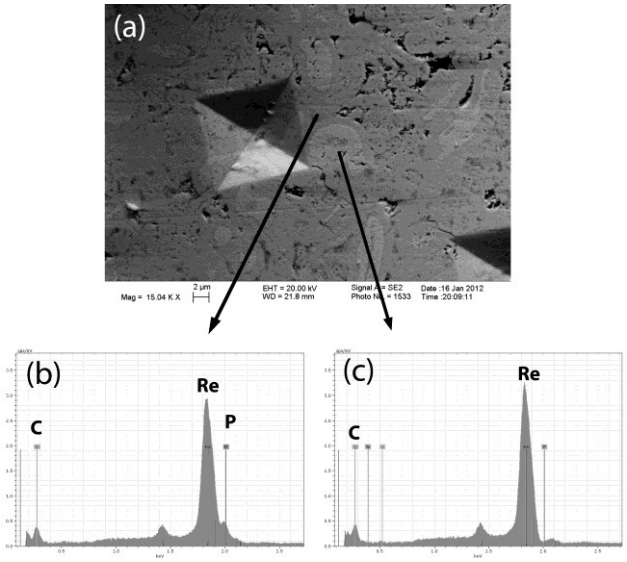

Figure 6. (a) SEM image of sample surface with 0.2 Vickers indent (d = 17.1 μm). Pores (black contrast) are visible in the upper right part of the image. As evidenced by local EDX analysis at the locations indicated by the arrowheads, the darker grey material contains Re and P in a 2:1 ratio (spectrum (b)), whilst the lighter, and slightly harder material appears to be completely depleted of P (spectrum (c)). Additional carbon is present in both materials.

With a hardness around 13 GPa, Re_2P is in the same range as zirconia (ZrO_2) ceramic, exceeds the hardness of elemental, metallic rhenium,[17] and is considerably harder than hardened steel. Given the high bulk modulus of Re_2P, its hardness is however quite low, if, for example compared to tungsten carbide WC, which exhibits a high bulk modulus of B_0 = 421 GPa and a hardness in the range of 30 GPa.[10]

However, Re_2P is in very good agreement to other refractory rhenium compounds like Re_2C or ReB_2, which have also extremely high bulk moduli but show a relatively small hardness.[11,49–52] The low hardness can be expected to be a direct consequence of the metallic properties of Re_2P (see chapter D) resulting in lower activation barriers for plastic deformation. Additionally, the comparatively low hardness of ReB_2 was attributed to shear-induced structural transformation and plasticity,[53] which might also play a role in the case of Re_2P (or the composite), as the deformation mode in hardness measurements is always associated with both, compression and shear.

Magnetic and conductive properties. All known rhenium phosphides are black with metallic luster and therefore exhibit distinct magnetic and conductive behaviour (see Table 3). However, the physical properties of Re_2P have not been determined yet. Magnetic measurements reveal that Re_2P is Pauli-paramagnetic (see Figure 7). Its conductivity curve decreases with higher temperatures as is typical for metals (see Figure S1).

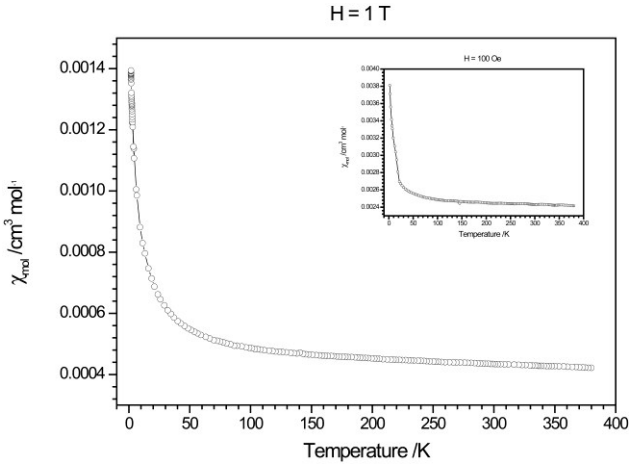

Figure 7. Evolution of molar susceptibility with temperature for Re_2P at an applied external field of 1 T (10^4 Oe) and 100 Oe (upper right).

The specific resistance and conductivity at ambient temperature were measured to be $5.0(4)\cdot10^{-6}$ Ωm and $0.2(1)\cdot10^{6}$ $\Omega^{-1}m^{-1}$, respectively. The latter value is significantly lower than that of elemental rhenium, which is around $5.5\cdot10^{6}$ $\Omega^{-1}m^{-1}$.[53] This observation is in good agreement with the expected electrical behavior.

Table 3. Magnetic and conductive properties of rhenium phosphides.

	Magnetic behavior	Electrical conductivity	Literature
Re_2P	Pauli-paramagnetic	metallic	this work
Re_3P_4	diamagnetic	semimetallic	[18]
Re_6P_{13}	paramagnetic	metallic	[54,55]
$ReP_{2.3}$	paramagnetic	unknown	[18]
Re_2P_5	diamagnetic	semiconducting	[55]
ReP_3	diamagnetic	unknwon	[56]
ReP_4	diamagnetic	semiconducting	[18]

Thermal behaviour. The temperature-dependent *in situ* X-ray powder diffraction patterns of Re_2P are shown in Figure 8.

Re_2P is stable up to 1250 K and exhibits an averaged thermal expansion of $32.8(2)\cdot10^{-6}$ K^{-1} (see Table 4). All cell parameters increase linearly with increasing temperature. The average thermal expansion shows nearly isotropic behavior.

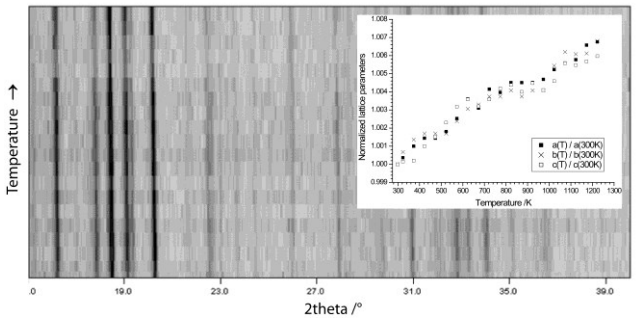

Figure 8. Temperature-dependent *in situ* X-ray powder diffraction patterns (Mo-$K_{\alpha1}$) of Re_2P and evolution of lattice parameters with temperature (upper right).

Table 4. Average linear and volumetric thermal expansion coefficients of Re_2P obtained by analysis of temperature-dependent *in situ* X-ray powder diffraction patterns from 300 to 1250 K.

Lattice parameter/cell volume	α / 10^{-6} K^{-1}
a	8.5(1)
b	7.9(2)
c	9.1(3)
V	32.8(2)

The automatically measured relative expansion $\Delta L/L$ of sintered Re_2P obtained by dilatometry is about 0.85 % over the estimated temperature interval of 250–1250 K yielding a thermal expansion coefficient of $28.5\cdot10^{-6}$ K^{-1}. This value is in good agreement with the data of the analysis of the temperature-dependent *in situ* X-ray powder diffraction patterns.

The thermal expansion coefficient of Re_2P is comparable with those of likewise metallic materials[57] and unfortunately exceeds those of ceramic compounds which have a variety of applications in industry.

Conclusion

By *in situ* high-pressure experiments on Re_2P in a diamond-anvil cell at ESRF and DESY up to 37.0 GPa, we were able to determine its bulk modulus and first pressure derivative by fitting a second- and third-order BM-EoS to the experimental *p*–*V* data. These data were compared to the values obtained from an Eulerian strain versus normalized stress plot resulting in an overall bulk modulus of 320(10) GPa. The experimental data were confirmed by theoretical calculations classifying Re_2P amongst the ultra-incompressible materials. In contrast, hardness measurements revealed a Vickers hardness of only 13(2) GPa in the asymptotic hardness region for a Re_2P-Re_xC_y composite material. Thus, in spite of the very high bulk modulus and the pronounced metallic character ($\sigma_{specific} = 0.2(1)\cdot10^6$ $\Omega^{-1}m^{-1}$) we claim anisotropic force loads of the indenter and possibly shear-induced phase transformation as with ReB_2 are responsible for the comparatively low hardness of Re_2P. Temperature-dependent *in situ* X-ray diffractometry reveals that Re_2P shows an approximately isotropic expansion of the lattice parameters with temperature. Its thermal expansion coefficient of $\alpha(V) = 28.5–32.8(2)\cdot10^{-6}$ K^{-1} is typical for metals and metallic compounds.

ASSOCIATED CONTENT

Supporting Information. Table S1 with details of the Rietveld refinements and crystallographic data for Re_2P at ambient conditions and at 37.0 GPa (DESY); Comments on the microstructure and composition of as-sintered Re_2P; Figure S1 with specific conductivity and resistance of Re_2P versus temperature.

AUTHOR INFORMATION

Corresponding Author

* wolfgang.schnick@uni-muenchen.de

ACKNOWLEDGMENT

The authors would like to thank ESRF and DESY for access to their instruments and support during the beamtime. Portions of this research were carried out at the light source PETRA III at DESY, a member of the Helmholtz Association (HGF). We would like to thank for using beamline P02.2. In addition, the authors would also like to thank Rainer Frankovsky (magnetic and conductivity measurements) and Thomas Miller (temperature-dependent *in situ* X-ray diffractometry), both at LMU Munich, as well as Natalia Smolskaia (hardness testing and sample preparation) from TU Bergakademie Freiberg and NETZSCH Applikationslabor (mechano-thermal analysis) at Selb, Germany. Financial support from the Fonds der Chemischen Industrie (FCI) and the Deutsche Forschungsgemeinschaft (DFG) within SPP 1236 (project SCHN 377/13-2) and BMBF (project 05K10RFA) is gratefully acknowledged.

REFERENCES

(1) Fantsichev, I. N.; Voronov, F. F.; Bokuta, S. A. *Elastic Constants and Elastic Moduli of Metals and Insulators: Handbook*; Naukova Dumka, Kiev, 1982.
(2) Novikov, N. V. *Physical Properties of Diamond: Handbook*; Naukova Dumka, Kiev, 1987.
(3) Clerc, D. G.; Ledbetter, H. M. *J. Phys. Chem. Solids* **1998**, *59*, 1071.
(4) Teter, D. M. *Mater. Res. Soc. Bull.* **1998**, *23*, 22.
(5) Kislyi, P. S. *Superhard and Refractory Materials*; Institute of Superhard Materials, Kiev, 1985.
(6) Aleksandrov, I. V.; Goncharov, A. F.; Makarenko, I. N.; Zisman, A. N.; Yakovenko, E. V.; Stishov, S. M. *High Press. Res.* **1989**, *1*, 333.
(7) Aleksandrov, I. V.; Goncharov, A. F.; Zisman, A. N.; Stishov, S. M. *Zh. eksp. teor. Fiz.* **1987**, *93*, 680.
(8) Cumberland, R. W.; Weinerger, M. B.; Gilman, J. J.; Clark, S. M.; Tolbert, S. H.; Kaner, R. B. *J. Am. Chem. Soc.* **2005**, *127*, 7264.
(9) Pierson, H. O. *Handbook of Refractory Carbides and Nitrides*; Noyes Publication, Westwood, New Jersey, 1996.
(10) Brazhkin, V. V.; Lyapin, A. G. *Phils. Mag. A* **2002**, *82*, 231.
(11) Juarez-Arellano, E. A.; Winkler, B.; Friedrich, A.; Wilson, D. J.; Koch-Müller, M.; Knorr, K.; Vogel, S. C.; Wall, J. J.; Reiche, H.; Crichton, W.; Ortega-Aviles, M.; Avalos-Borja, M. *Z. Kristallogr.* **2008**, *223*, 492.
(12) Ono, S.; Kikegawa, T.; Ohishi, Y. *Solid State Commun.* **2005**, *133*, 55.
(13) Young, A. F.; Sanloup, C.; Gregoryanz, E.; Scandolo, S.; Hemley, R. J.; Mao, H.-k. *Phys. Rev. Lett.* **2006**, *96*, 155501.

(14) Crowhurst, J. C.; Goncharov, A. F.; Sadigh, B.; Evans, C. L.; Morrall, P. G.; Ferreira, J. L.; Nelson, A. J. *Science* **2006**, *311*, 1275.
(15) Gregoryanz, E.; Sanloup, C.; Somayazulu, M.; Badro, J.; Fiquet, G.; Mao, H.-k.; Hemley, R. J. *Nature Mater.* **2004**, *3*, 294.
(16) Friedrich, A.; Winkler, B.; Bayarjargal, L.; Morgenroth, W.; Juarez-Arellano, E. A.; Milman, V.; Refson, K.; Kunz, M.; Chen, K. *Phys. Rev. Lett.* **2010**, *105*, 085504.
(17) Wern, H. Single crystal elastic constants and calculated bulk properties; Logos Verlag, Berlin, 2004.
(18) Rühl, R.; Flörke, U.; Jeitschko, W. *J. of Solid State Chem.* **1984**, *53*, 55.
(19) Mezouar, M.; Crichton, W. A.; Bauchau, S.; Thurel, F.; Witsch, H.; Torrecillas, F.; Blattmann, G.; Marion, P.; Dabin, Y.; Chavanne, J.; Hignette, O.; Morawe, C.; Borel, C. *J. Synchrotron Radiat.* **2005**, *12*, 659.
(20) Boehler, R.; DeHantsetters, K. *High Press. Res.* **2004**, *24*, 391.
(21) Mao, H.-k.; Xu, J.; Bell, M. J. *Geophys. Res.* **1986**, *91*, 4673.
(22) Hammersley, A. P.; Svensson, S. O.; Hanfland, M.; Fitch, A. N.; Hausermann, D. *High Press. Res.* **1996**, *14*, 235.
(23) Liermann, H.-P.; Morgenroth, W.; Ehnes, A.; Berghäuser, A.; Winkler, B.; Franz, H.; Weckertm, E. The Extreme Conditions Beamline at PETRA III, DESY: Possibilities to conduct time resolved monochromatic diffraction experiments in dynamic and laser heated DAC; 22nd AIRAPT Conference: J. Phys.: Conf. Series, accepted for publication 2010.
(24) R. Letoullec, J. P. Pinceaux, and P. Loubeyre, High Press. Res. **1**, 77 (1988).
(25) Dera, P. GSE_Shell, Data analysis program for monochromatic powder diffraction with area detector, GeoSoilEnviro Consortium for Adv. Radiat. Sources, Chicago, 2008.
(26) Coelho, A. A. *TOPAS-Academic*, Version 4.1, Coelho Software, Brisbane, 2007.
(27) Bergmann, J.; Kleeberg, R.; Haase, A.; Breidenstein, B. *Mater. Sci. Forum* **2000**, *347–349*, 303.
(28) Birch, F. *Phys. Rev.* **1947**, *71*, 809.
(29) Murnaghan, F. Proc. Natl. Acad. Sci. USA **1944**, 30, 244.
(30) Heinz, D. L.; Jeanloz, R. *J. Appl. Phys.* **1984**, *55*, 885.
(31) Origin 6.1, v6.1052 (B232), OriginLab Corporation, 2000.
(32) Clark, S. J.; Segall, M. D.; Pickard, C. J.; Hasnip, P. J.; Probert, M. J.; Refson, K.; Payne, M. C. *Z. Kristallogr.* **2005**, *220*, 567.
(33) *CASTEP User Guide*; Accelrys Inc. San Diego, 2008.
(34) Milman, V.; Winkler, B.; White, J. A.; Pickard, C. J.; Payne, M. C.; Akhmatskaya, E. V.; Nobes, R. H. *Int. J. Quantum Chem.* **2000**, *77*, 895.
(35) Perdew, J. P.; Ruzsinszky, A.; Csonka, G. I.; Vydrov, O. A.; Scuseria, G. E.; Constantin, L. A.; Zhou, X.; Burke, K. *Phys. Rev. Lett.* **2008**, *100*, 136406.
(36) Monkhorst, H. J.; Pack, J. D. *Phys. Rev. B* **1976**, *13*, 5188.
(37) Walker, D.; Carpenter, M. A.; Hitch, C. M. *Am. Mineral.* **1990**, *75*, 1020.
(38) Huppertz, H. *Z. Kristallogr.* **2004**, *219*, 330.
(39) Rubie, D. C. *Phase Transitions* **1999**, *68*, 431.
(40) Kawai, N.; Endo, S. *Rev. Sci. Instrum.* **1970**, *8*, 1178.
(41) Rundqvist, S. *Acta Chem. Scand.* **1960**, *14*, 1961.
(42) Sims, C. T.; Craighead, C. M.; Jaffee, R. I. *Naturwissenschaften* **1931**, *19*, 575.
(43) Bull, S. J.; Page, T. F.; Yoffe, E. H. *Phil. Mag. Lett.* **1989**, *59*, 281.
(44) Li, H.; Bradt, R. C. *J. Mater. Sci.* **1993**, *28*, 917.
(45) Tabor, D. *The hardness of metals*; Clarendon Press, Oxford, 1951.
(46) McColm, I. J. *Ceramic Hardness*; Plenum Press, New York, 1990.
(47) Fröhlich, F.; Grau, P.; Grellmann, W. Phys. *Status Solidi A* **1977**, *42*, 79.
(48) Hirao, K.; Tomozawa, M. *J. Am. Ceram. Soc.* **1987**, *70*, 497.
(49) Chung, H.-Y.; Weinberger, M. B.; Levine, J. B.; Kavner, A.; Yang, J.-M.; Tolbert, S. H.; Kaner, R. B. *Science* **2007**, *316*, 436.
(50) Dubrovinskaia, N.; Dubrovinsky, L.; Solozhenko, V. L. *Science* **2007**, *318*, 1550c.
(51) Chung, H.-Y.; Weinberger, M. B.; Levine, J. B.; Cumberland, R. W.; Kavner, A.; Yang, J.-M.; Tolbert, S. H.; Kaner, R. B. *Science* **2007**, *318*, 1550d.
(52) Zhang, R. F.; Legut, D.; Niewa, R.; Argon, A. S.; Veprek, S. *Phys. Rev. B* **2010**, *82*, 104104.
(53) Bass, J. Electrical resistivity of pure metals and dilute alloys; Springer, Berlin, 1980.
(54) Guérin, R.; Potel, M.; Sergent, M. *Mater. Res. Bull.* **1979**, *14*, 1335.
(55) Rühl, R.; Jeitschko, W. *Inorg. Chem.* **1982**, *21*, 1886.
(56) Rühl, R.; Jeitschko, W. *Acta Crystallogr. Sect. B* **1982**, *38*, 2784.
(57) Lide, D. R. *Handbook of Chemistry and Physics*; CRC Press, Boca Raton, 2008.

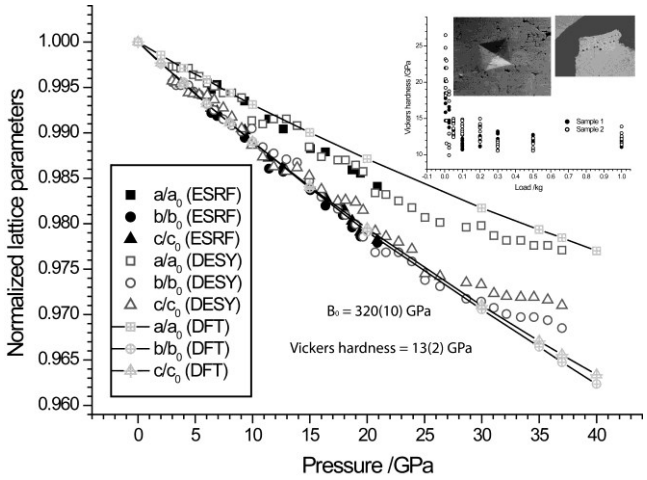
Normalized lattice parameters
Pressure /GPa
a/a0 (ESRF)
b/b0 (ESRF)
c/c0 (ESRF)
a/a0 (DESY)
b/b0 (DESY)
c/c0 (DESY)
a/a0 (DFT)
b/b0 (DFT)
c/c0 (DFT)
B0 = 320(10) GPa
Vickers hardness = 13(2) GPa
Vickers hardness /GPa
Load /kg
Sample 1
Sample 2